Auxosporulation and Cell Enlargement in Thalassiroid Diatoms

By

Emma Farrell

A thesis submitted to the Department of Biology

Mount Allison University

in partial fulfillment of the requirements for the

Bachelor of Science degree with Honours

May 6th, 2020

Contents

Figures and Tables

1 Abstract

Our understanding of diatom reproduction is limited, especially for marine planktonic centric diatoms. This project aimed to observe sexual behavior and auxospore development in the polar centric group, Thalassiosirales, that maintains the morphology of a nonpolar centric diatom. Auxosporulation is the main means of restoring large cell sizes in the majority of diatom species examined. Monoclonal cultures of *T. weissflogii* (CCMP1587), *T. nordenskioeldii* (CCMP997) and *Thalassiosira* cf. *oceanica* were subjected to sexual induction protocols, resulting in non-typical cells. Spermatogenesis was not observed and presumed absent in all inductions. Spherical cells with non-siliceous cell walls were observed, occurring in about 12% of the population for *T. nordenskioeldii*, and 17% in *T. weissflogii*. However, these spherical cells were not eggs or auxospores and further observations using light microscopy (LM) suggest that these cells were arrested in this stage of enlargement and eventually died. Spherical and irregular shaped cells were observed in *T. weissflogii*, as well as cells in general appearance similar to auxospores. The nuclear behavior observed in T. *weissflogii* indicates that this species could reproduce via autogamy, but mature initial cells enclosed within such “auxospores” were never observed. Inductions were not successful in *Thalassiosira* cf. *oceanica.* In the absence of gametogenesis and mature auxospores, the larger typical vegetative cells encountered in cultures following induction protocols in *T. nordenskioeldii* and *T. weissflogii* are therefore attributed to vegetative cell enlargement.

Key words: *auxosporulation, diatoms, cell enlargement, Thalassiosirales*

2 Introduction

Diatoms are a species-rich and productive group of eukaryotic algae, which could be responsible or 20% of all photosynthetic fixation of carbon, therefore, playing an important role in water ecosystems (Chepurnov et al. 2004). They are a monophyletic group of unicellular eukaryotes, the majority of which are photoautotrophic with the distinguishing feature of a complex, siliceous cell wall named the frustule. In the diatom population, there are high levels of genetic variation which could be caused by this group's success in adapting to changing environmental conditions (Chepurnov et al. 2004). To understand the evolutionary success of diatoms, one must understand their life cycles, more specifically, their sexual reproduction. Diatoms have a unique life cycle as it is one of a very few algae groups that have a diplontic life cycle with two main stages: diploid vegetative and haploid sexual (Mills and Kaczmarska 2006; Chepurnov et al. 2004; Round et al. 1990). As the population propagates asexually through mitotic division, in which the frustule of one of the daughter cells is smaller. This, therefore, causes the average size of the cell in such population decreases progressively, commonly referred to as "diatom cell diminution" (Round et al. 1990). Restoration of larger cell sizes and their reintroduction to local populations, is an obligate part of the life cycle of most diatoms and is typically achieved by sexual reproduction that results in production of the auxospore and the initial cell; the latter is a product of the auxospore and is a large diploid cell capable of resuming mitotic division and diatom cell diminution. Centric diatoms are commonly oogamous, which involves the fertilization of a large, "egg" by a small, uniflagellated sperm.

Gametes are formed though gametogenesis, which is a process by which gametes are formed within a gametangium (Kaczmarska et al. 2013). Since diatoms are diplonts, gametogenesis always includes meiosis (Kaczmarska et al. 2013). There are two types of gametogenesis that occur in centric diatoms, one that produces "egg cells" while the other produces uniflagellated sperm or non-flagellated spermatia (Davidondich et al. 2017). In diatoms, an egg cell is formed in a parent individual which converts to an oogonium. The oogonium also eventually becomes a primary oocyte and undergoes meiosis, which is a cell whose nucleus will enter meiosis producing one tri-nucleated or two bi-nucleated "eggs" (Kaczmarska et al. 2013). There are three distinct patterns of oogenesis that differ due to the number of eggs and polar bodies produced (Kaczmarska et al. 2013; Mizuno 2006). Type one

oogenesis occurs when the oocytes undergo normal cytokinesis following meiosis I, and produces two bi-nucleated eggs. Type two oogenesis is very similar to type one, however, cytokinesis is unequal, producing one bi-nucleated egg cell and a polar body that later degenerates (Kaczmarska et al. 2013; Mizuno 2006). In type three oogenesis, meiosis I proceeds without cytokinesis, and one nucleus aborts (or pyknotises) and then the following meiosis II is acytokinetic and leads to the abortion of one of the haploid nuclei, thus, producing only one tri-nucleated egg cell (Kaczmarska et al. 2013; Mizuno 2006). This type of oogenesis is commonly observed in the order Thalassiosirales, notably in the genera *Thalassiosira*, *Cyclotella*, and *Skeletonema* (Mizuno 2008). Spermatogenesis is much more variable and complex than oogenesis. It begins with a series of differentiating mitotic divisions, during which, these resulting cells do not grow, as in normal mitosis (Samanta et al. 2018; Kaczmarska et al. 2013). Spermatogenesis begins with a diploid primary spermatocyte that undergo meiosis to produce four uninucleate, uniflagellate gametes (sperm) in a two-step meiosis with no nuclei abort, which is different from oogenesis (Manton 1966; Kaczmarska et al. 2013). Sperm formation can either be merogenous or hologenous. The merogenous type, the colorless spermatids bud from the plastid containing spermatocytes after meiosis II, leaving only one or two residual bodies (Samanta et al. 2018). In hologenous sperm formation, the primary spermatocyte is divided among the four sperm. Typically, this division begins when the primary spermatocyte divides to form two haploid secondary spermatocytes after meiosis I. Then it further divides to produce two haploid spermatids, which differentiate into sperm (Kaczmarska et al. 2013). Spermatogenesis is highly variable, especially within families. For example, in the order Thalassiosirales spermatogenesis in *Thalassiosira punctigera* is merogenous, while in *Cyclotella meneghiniana* it is hologenous (Mizuno 2008). Once the two gametes combine their genetic material, the auxospore develops, which will nurture the enlarging protoplast and eventually reinstate the large initial cell frustule. Which then reproduces with meiotic division once again. This life cycle for centric diatoms is shown below in Figure 1.

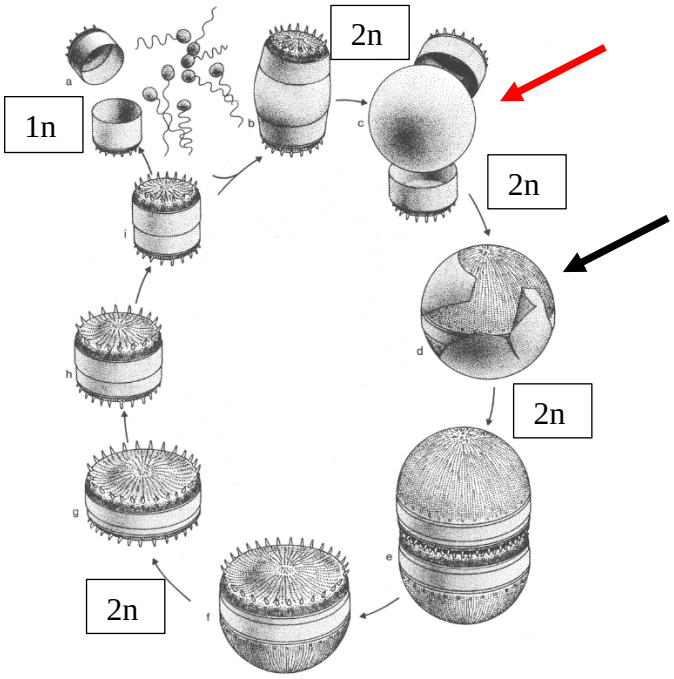

Figure 1. Life cycle of a typical centric diatom showing the haploid (1n) sexual stage and the diploid (2n) vegetative stage (Round et al. 1990). The red arrow is pointing the immature auxospore, while the black arrow is pointing to the mature auxospore containing the initial cell.

Auxosporulation is a complex process (encompassing sexualization, gametogenesis, and auxospore production and development, and initial cell formation) and it has been observed across taxa, providing insights into deep relationships among the diatoms (von Stocsh 1982; Kaczmarska et al. 2013). Auxospore growth patterns and cell wall structures are used to define major diatom groups. Auxospores that grow isodiametrically, growing evenly in all directions, with only siliceous scales in their walls are typical of the nonpolar centric diatoms. On the other hand, auxospore growth in polar diatoms (polar centrics and pennates) is anisodiametric due to walls containing perizonial bands that effect the valve polarity of the initial cell.

Originally, scientists assumed that diatoms could be divided into two groups that were determined by their process of sexual reproduction and valve patterning centers (Round et al. 1990). The centric diatoms were found oogamous with radially organized patterning on their valves and were distinct from the then thought all to be isogamous pennate diatoms that had bilateral valve face pattern organization. The pennates were further divided into two classes based on the presence of a raphe (Round et al. 1990). However, while molecular evidence suggests that there are also three clades, they are not organized in the way that Round et al.

(1990) once thought. Instead ‘Class 1’ contains the nonpolar centric diatoms with circular valve shape and radial valve patterning (Coscinodiscophyceae). Polar diatoms have two classes: one with polar centrics, and the radial Thalassiosirales (Mediophyceae) and the other with the pennates who are polar by default (Bacillariophyceae) (Medlin and Kaczmarska 2004; Medlin 2016). This molecular phylogeny indicated that there is a group of morphologically nonpolar centric diatoms, Thalassiosirales, that are actually embedded in polar centrics, class Mediophyceae (Kaczmarska et al. 2001; Medlin and Kaczmarska 2004; Medlin 2016). The valve polarity of Mediophyceae (with Thalassiosirales as the exception) is affected by the perizonial bands shaping the auxospore wall which facilitates uneven growth, making a variety of valve morphologies (Kaczmarska et al. 2001; Medlin 2016); the bands are absent in Thalassiosirales.

The members of the order Thalassiosirales, not only share similar morphology but sexual reproduction as well with nonpolar diatoms with isometric auxospore growth and oogamous reproduction, as observed in *Thalassiosira punctigera* and *Skeletonema marioni* (Mills and Kaczmarska 2006; Godhe et al. 2014), and others. However, the diversity in the sexual reproduction within this order suggest that complexity is present, therefore supporting the new phylogeny that indicates this order is more closely related to nonpolar centric diatoms. Schultz and Trainor (1970) observed abnormal cell development in *Cyclotella* and documented that the protoplast was not fully contained and would swell from the upper valve and form a new upper valve on the free surface. This process created a series of upper valves which is irregular in any auxospore formation that is expected in the order of Thalassiosirales. Normally anywhere from one to two (sometimes 3) valves will form inside the auxospore. However, these typical valve formations were also observed, e.g., in other *Thalassiosira* species (Mills and Kaczmarska 2006; Chepurnov et al. 2006). Two-step auxosporulation has also been observed within this order, in the species *Thalassiosira punctigera.* Two-step auxosporulation occurs when the initial cells formed by small-celled oogonia are not the maximum size for the species. Either the cells become vegetative and begin mitotic divisions or the cells become resexualized and function as a larger oogonia (Chepurnov et al. 2006). Two-step auxosporulation is rare in centric diatoms and is not often recognized, which may suggest diversification of the order Thalassiosirales from other nonpolar centric groups.

This study attempted sexualization of three species from the order Thalassiosirales in order to expand our knowledge of auxosporulation in Thalassiosirales, and gain understanding of the evolutionary history of these diatoms. Notably, to better understand the new placement of Thalassiosirales in molecular phylogenies. The specific aim of this study is twofold. First, the progress of full sexualization in *Thalassiosira* spp. is observed using modern microscopical methods such as SEM, EDS, and fluorescence. There is a strong focus to the later stages of induced cell development and the cell wall structure. Secondarily is the development of observed large cells in my cultures of three species of *Thalassiosira*. This development will be compared to the development of other centric diatom species.

3 Methods and methods

3.1 Stock cultures

A monoclonal culture of *Thalassiosira nordenskioeldii* (CCMP 997) and *Thalassiosira weissflogii,* (CCMP 1587) were purchased from the Bigelow Laboratory in Maine. CCMP 997 was collected in Norway and isolated by E. Syvertsen. CCMP 1587 was collected by Q. Adnan in Indonesia, and isolated by P. Hargraves. Our own clone, PicoThala (*Thalassiosira* cf. *oceanica*), was isolated from Saint Andrews in the Passamaquoddy Bay. The stock was grown in f/2 with additional silica (Guillard 1975) for all cultures in 125 mL flasks, which were inoculated into new flasks every three to four weeks in order to maintain exponential growth. CCMP 997 was grown in 5 °C in 24:0 h light:dark cycles and at illumination levels of 6 μmol $s^{-1}m^{-2}$ and 10 °C in 12:12 h light:dark cycles at illumination levels of 20 μmol $s^{-1}m^{-2}$. CCMP 1587 and PicoThala were grown in 10-15 °C in 12:12 light:dark cycles at illumination levels of 20 μmol $s^{-1}m^{-2}$. Light levels were measured using a model LI-250 light meter (LI-COR Bioscience, Lincoln, Nebraska, USA).

3.2 Microscopical Examinations

Light Microscope (LM) and Sampling

Following the induction trial, the cultures were examined for the presence of sexual cells by using a Zeiss Axiolab light microscope (LM). The cells were imaged using a digital camera

(Zeiss AxioCam ICc3). The diameter of the cells' valve face was measured by dmFMeasuring software (Digital Measuring Microscopy Facility© Ehrman) to determine size classes from images taken daily. The culture was observed daily until the experiment was complete. PDMPO (2-(4-pyridyl)-5-((4-(2-dimethylaminoethylaminocarbamoyl)methoxy)phenyl)oxazole), a silica specific fluorescent dye was added to the batch culture flasks, with a final working concentration of 1 μM using protocol outlined by Znachor and Nedoma (2008), added after the first day of experiments, to track newly deposited biogenic silica in frustules. Every few days, or when an important sexual stage, such as gametogenesis or auxospores were anticipated, the experimental batch culture was sampled and fixed for epifluorescence light microscopy (ELM) and scanning electron microscopy (SEM). These samples were fixed with 2.5% glutaraldehyde fixative that was prepared from 25% EM grade glutaraldehyde that was added to 90 mL of autoclaved seawater.

Staining and Epifluorescence microscopy

To visualize nuclei during auxosporulation, the fixed samples were stained with Vectashield Mounting Medium with DAPI (Vector Laboratories, Burlingame, CA, USA) and observed under Zeiss Axioskop 2 Plus (Carl Zeiss, Oberkochen, Germany) fluorescence light microscope with an Excelitas X-cite (Excelitas Technologies, Massachusetts, United States) LED illuminator. Images were taken that an AxioCam color camera that was fitted to the microscope (Carl Zeiss, Gottingen Germany).

Scanning Electron Microscope (SEM): Confirming Identification of Clones

To confirm the identity of the clones, few weeks after their arrival, about 1-3 mL of the stock cultures were placed in a hot acid bath containing a 1:1 ratio of nitric acid: sulfuric acid solution for 20 minutes. The samples were then filtered, using 3μm filter paper, which then was set out to dry. The filters were then mounted onto aluminum stubs with double sided tape and coated with gold using Anatech Hummer 6.2 sputtering system (Anatech USA, Nevada) powered by argon as a source gas. Once mounted and coated, the samples were examined using Hitachi SU3500 SEM (Hitachi High-Tech Global) operating at 10kV and 5 mm working distance. During SEM observation, 10 images of the outside view and 10 of the inside view of the valves

were taken for each clone. Standard diagnostic characters, such as the two orthogonal diameters which will be further referred as mean diameters, as well as the number of fultoportula and areolae (in 10 μm) on the valve face were measured using the dMFMeasure software (Digital Microscopy Facility). These values were compared to the species specific cell size ranges for the species of this genus outlined in Tomas (1997).

Auxospores and other soft walled cell structures using SEM and Energy-dispersive X-ray spectroscopy (EDS)

To examine the cell wall structure of the non-typical cells found following the induction, some of the glutaraldehyde fixed samples were rinsed on filter paper and then soaked in 1% aqueous osmium tetroxide for one hour of soaking. Next, the samples were dehydrated in a graded ethanol series (35%, 50%, 75%, 95%, 100%) for 10 minutes at each step. To minimize cell collapse of the soft-walled cells, they were dried using critical point drying (CPD). The filter with cell material was loaded into the Denton CPD-1 (Denton Vacuum, New Jersey, United States) critical point dryer and four, 2-minute exchanges of CO2 were performed. At the ten-minute mark, room temperature water was placed in the chamber, surrounding the filter chamber (pressure 900 psi), then replaced by hot tap water (pressure 1500psi) for ten minutes. Afterwards, the chamber was vented, returning the tank pressure to 0 psi over a twenty-minute time period. The CPD samples were then mounted and coated with gold to observe using Hitachi SU3500 SEM (Hitachi High-Technologies, Toronto).

3.3 Sexual Induction

CCMP 997 (Thalassiosira nordenskioeldii)

To induce my diatom batch culture populations to reproduce sexually the light intensity and temperature were manipulated. CCMP 997 (***Thalassiosira nordenskioeldii)*** was subjected to the sexual induction protocol similar to that of Mills and Kaczmarska (2006). In total, four experiments were conducted on 4 different batch cultures of CCMP 997 using combination of different light and temperature conditions as well as different batch culture ages. These experiments and their parameters are shown in Tables 1 and 2. After 4 days of treatment, each

flask was returned to normal growth conditions and observed using LM for one week to observe cell development of induced cells.

Table 1. Induction I. Sexual Protocol for CCMP 997 for experiments 1 (4 weeks old) and 3 (2 weeks old) with two different inoculation ages, acclimated to 5℃.

	L:D	Intensity (light)	Temp	Media
Day 0	24:0	6.65 µE	4-6℃	f/2 + Si
Day 1	24:0	89.68 µE	10-12℃	f/2 + Si
Day 2	24:0	89.69 µE	10-12℃	f/2 + Si
Day 3	0:24	0 µE	4-6℃	f/2 + Si
Day 4	0:24	0 µE	4-6℃	f/2 + Si
Day 5 - 10	24:0	6.65 µE	4-6℃	f/2 + Si

Table 2. Induction II. Sexual Protocol for CCMP 997 for experiments 2 (4 weeks old) and 4 (2 weeks old) with two different inoculation ages, acclimated to 10℃.

	L:D	Intensity (light)	Temp	Media
Day 0	24:0	20 µE	10℃	f/2 + Si
Day 1	24:0	89.68 µE	5℃	f/2 + Si
Day 2	24:0	89.69 µE	5℃	f/2 + Si
Day 3	0:24	0 µE	10℃	f/2 + Si
Day 4	0:24	0 µE	10℃	f/2 + Si
Day 5 - 10	24:0	20 µE	10℃	f/2 + Si

CCMP 1587 (Thalassiosira weissflogii) and PicoThala (Thalassiosira sp.)

To induce my diatom populations to reproduce sexually, clones, *Thalassiosira* cf. *oceanica* (PicoThala) and *Thalassiosira weissflogii* (CCMP 1587) were inoculated in f/2 with additional ammonium following the Moore et al. (2017) protocol. The media contained a working concentration of 800 µM of NH4Cl, by adding 800 µL of 1M NH4Cl solution to 1L of f/2 media before autoclaving. Both *T. weissflogii* and *T.* cf. *oceanica* were grown in 100 µE after they were reinoculated in the modified media in 15 ℃. Table 3 below shows the induction protocols for these experiments for the clones of *T. weissflogii* and *T.* cf. *oceanica*. The cultures were observed daily for 10 days and the cells were enumerated every 2 days.

Table 3. Induction III for CCMP 1587 and PicoThala using modified media.

	L:D	Intensity (light)	Temp	Media
Day 0	24:0	100 µE	15℃	f/2 + Si + NH4Cl
Day 1	24:0	100 µE	15℃	f/2 + Si + NH4Cl
Day 2	24:0	100 µE	15℃	f/2 + Si + NH4Cl
Day 3	24:0	100 µE	15℃	f/2 + Si + NH4Cl
Day 4-10	24:0	100 µE	15℃	f/2 + Si + NH4Cl

Another experiment, combining the Moore et al. (2017) which used newly inoculated flask in modified media, in combination to the Mills and Kaczmarska (2006) protocol similar to the one used for *Thalassiosira nordenskioeldii* with varying temperature and light conditions. This protocol is outlined in Table 4.

Table 4. Induction IV for CCMP 1587 and PicoThala using modified media and Mills and Kaczmarska (2006) light and temp protocol.

	L:D	Intensity (light)	Temp	Media
Day 0	12:12	20 µE	15℃	f/2 + Si + NH4Cl
Day 1	12:12	10 µE	12℃	f/2 + Si + NH4Cl
Day 2	12:12	10 µE	12℃	f/2 + Si + NH4Cl
Day 3	0:24	0 µE	12℃	f/2 + Si + NH4Cl
Day 4	0:24	0 µE	15℃	f/2 + Si + NH4Cl
Day 5	24:0	120.5 µE	15℃	f/2 + Si + NH4Cl
Day 6	24:0	120.5 µE	15℃	f/2 + Si + NH4Cl
Day 7-10	12:12	20 µE	15℃	f/2 + Si + NH4Cl

4 Results

4.1 Identification and Morphology of the diatom species examined

All clones examined here are centric diatoms, as their valve morphology is radial, and valve outline circular as indicated by the mean diameters. The clones can all be grouped in the genus *Thalassiosira* due to the discoid shape, loculate areolae arranged in rows, and fultoportulae arranged in a ring with typically one rimoportula (Round et al. 1990). Members of this genus can be either solitary (i.e. *Thalassiosira oceanica*) or joined by threads (*Thalassiosira nordenskioeldii*) (Round et al. 1990). The measurements of the cultured clones were compared to the valve size ranges of the suggested species for purchased clones, to confirm identification in Table 5 (Tomas 1997). My SEM images, showing both the inside and outside view of the valves, in Figure 2 are representative of the 60 images measured.

Table 5. Metric data for clones used obtained at the time of their arrival at the lab and those published by (Tomas 1997) for corresponding species.

	SVD	VD	VLA	MP	Source
Thalassiosira nordenskioeldii	-	10-50	14-18	3	Tomas 1997
CCMP 997	6-10	6-10	22-33	3-6	SEM Measurements
Thalassiosira weissflogii	-	5-32	30-40	9-16	Tomas 1997
CCMP 1587	5-7	5-7	20-73	12-23	SEM Measurements
Thalassiosira oceanica	-	3-12	40-60	3-4	Tomas 1997
PicoThala	3-4	3-4	24-94	9-11	SEM Measurements

SVD = Second measurement valve diameter (µm); VD = valve diameter (µm); VLA = number of stria areolae/10 µm on valve face; MP = number of marginal furtoportulae processes/10 µm).

Thalassiosira nordenskioeldii

T. nordenskioeldii Cleve (CCMP 997) has one marginal ring of strutted processes (or fultoportulae) with an average of 27 striae areolae/10 µm (SD =6.2, N=10) and a diameter of 7.8 µm (SD=1.7, N=20). It has prominent marginal rimoportula and a characteristically slanting

valve mantle (Fig 2, A-B). The characters fit within the widely accepted description of *T. nordenskioeldii*. However, even though the individual's valves were smaller or finer in ornamentation than average, given by Thomas (1997) for natural phytoplankton, my metrics overall agree/overlap with published data. The observed difference could be due to the age of the clone. CCMP 997 was originally isolated in 1978, and long-term culturing may have brought clone valves below what is seen in nature in this species.

Thalassiosira weissflogii

T. weissflogii Grunow (CCMP 1587) has an irregular ring-cluster of subcentral strutted processes (or fultoportulae). Its valves were on average of smaller diameter than *T. nordenskioeldii*, about 6.0 µm (SD=1.4, N=20). However, my clone of *T. weissflogii* may have a more stria areolae per 10µm on the valve face, which was 46 (SD=26.5, N=10) when compared to what is observed in nature, 30-40 (Tomas 1997). The marginal processes were arranged slightly more closely, with an average of 17.3 fultoportula/10 µm (SD=5.6, N=20), whereas 9-16 is what is commonly observed in natural populations (Tomas 1997). However, these physical feature averages still fall and overlap with the published range of *T. weissflogii*, coupled with the irregular areolation and small areolae (Fig 2, C-D).

Recently, *T. weissflogii* taxonomic affiliation was reappraised. Consequently, this and other similar species were moved to a separate genus as *Conticribra weissflogii* (Grunow) Stachura-Suchoples & D.M. Williams (Stachura-Suchoples and Williams 2009). The *Conticribra* genus is closely related to *Thalassiosira* genus but are separated by loculate areolae with continuous cribra and a non-plicated valve face in *Conticribra* (Stachura-Suchoples and Williams 2009) absent in *Thalassiosira*. However, this new genus has not yet been widely accepted. Therefore, the traditional species name of *T. weissflogii* is used here.

Thalassiosira sp.

Our clone, has the smallest cells of all the clones examined here, averaging at about 3.7 µm (SD=0.3, N=20) in diameter. It has marginal strutted processes, with an average of 10.5 fultoportulae per 10 µm (SD=1.4, N=20). The ornamentation on the valve face was fine, with an average 67.8 stria areolae per 10 µm (SD=35.7, N=10). This feature, coupled with the small cell

size and marginal ring of fultoportulae, suggest that this clone may be related to the species *Thalassiosira oceanica* Hasle (Fig 2, E-F). However, it is difficult to confirm this identity without genetic analysis, so this identification is tentative. Therefore, the abbreviation 'c.f.' is used in the species to reflect this degree of uncertainty in its identification. The observed stria areolae/10 µm on valve face of this clone (x= 68.7) is higher than what is observed in nature, 40-60, according to Tomas (1997). The largest difference between our clone PicoThala and *T. oceanica* is the ring of marginal furtoportulae/10 µm. PicoThala is nearly double, about 10.5 furtoportulae/10 µm (SD=1.4, N=10) than what is observed in nature for *T. oceanica* (3-4 furtoportulae/10 µm, Table 5). Despite this difference in the number of marginal furtoportuale, the clone PicoThala, is still fits best with *T. oceanica*. Therefore, the clone PicoThala will now be referred to as *Thalassiosira* cf. *oceanica*.

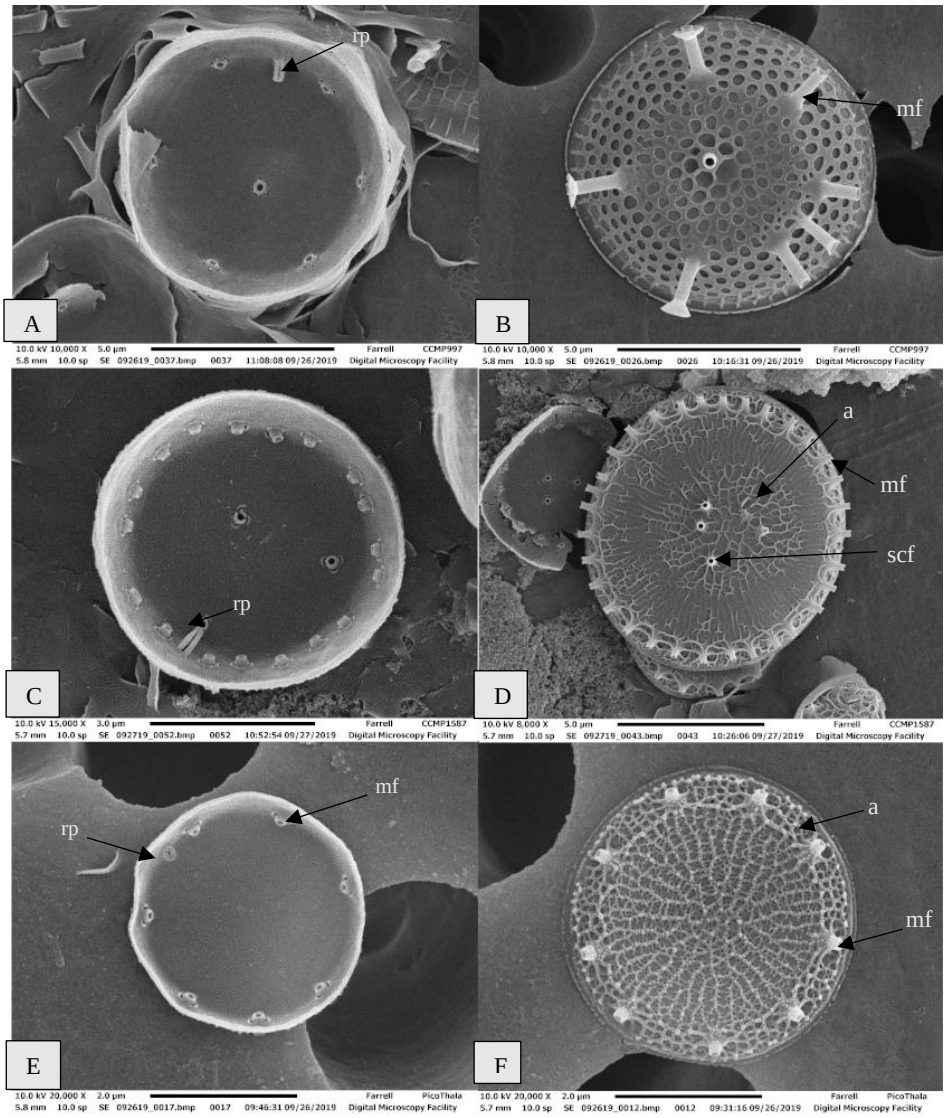

Figure 2. Inside (**A, C, E**) and outside (**B, D, F**), surface of vegetative valves. **A, B** Valve view of *T. nordenskioeldii*, showing prominent marginal fultoportula (mf) in outside view (B) and rimoportula (rp) in inside view (A). **C, D** Valve view of *Thalassiosira weissflogii* showing the ring of subcentral fultoportula (scf) and marginal fultoportula (mf) as well as the loculate areolae (a). **E, F** Valve view of *Thalassiosira* cf. *oceanica* showing the small areolae (a) of the valve face (k) and marginal ring of fultoportula (mf).

4.2 Induction of *T. nordenskioeldii*

Cell Types

Following the induction protocol, I and II, the first and free spherical cells, ranging from 30-50 µm, became evident on day 6 (Fig 3, A-B). Under the epifluorescence microscope, the PDMPO, which is a fluorescent dye that indicates the presence of silica (yellow), is not visible. Indicating these spherical cells do not have silica in their cell walls (Fig 4, B). Spermatogenesis was not observed in the cultures. However, free spherical cells that could have been either oocytes or eggs were present (Fig 3, C). However, these cells were very rare and since no auxospores or spermatogenesis was observed, it is unlikely that either oogenesis or auxospore production occurred. Small vegetative cells were commonly observed as well (Fig 3, D). Some of the post-induced cells were multinucleated as shown in Figure 4.

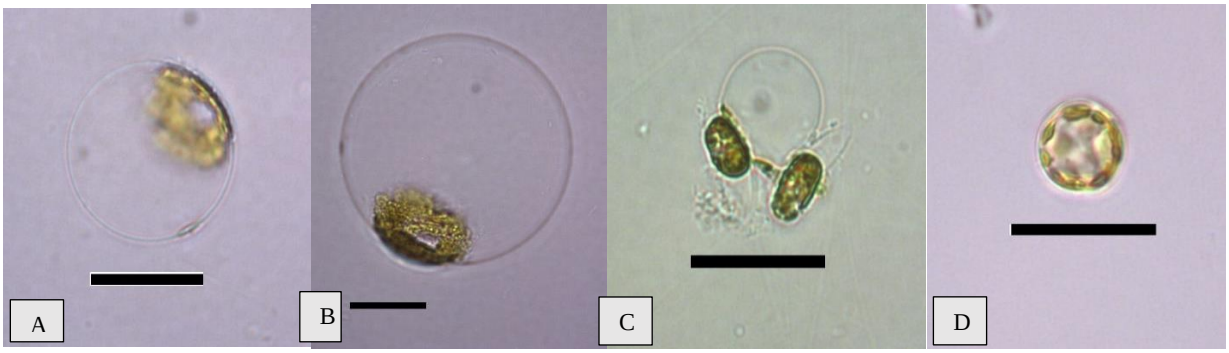

Figure 3. Atypical cells observed following induction of *T. nordenskioeldii.* (A, B) Enlarged spherical cells. (C) Disintegrating possible oocyte/egg. (D) Vegetative cell pre-induction. Scale bar = 25 µm.

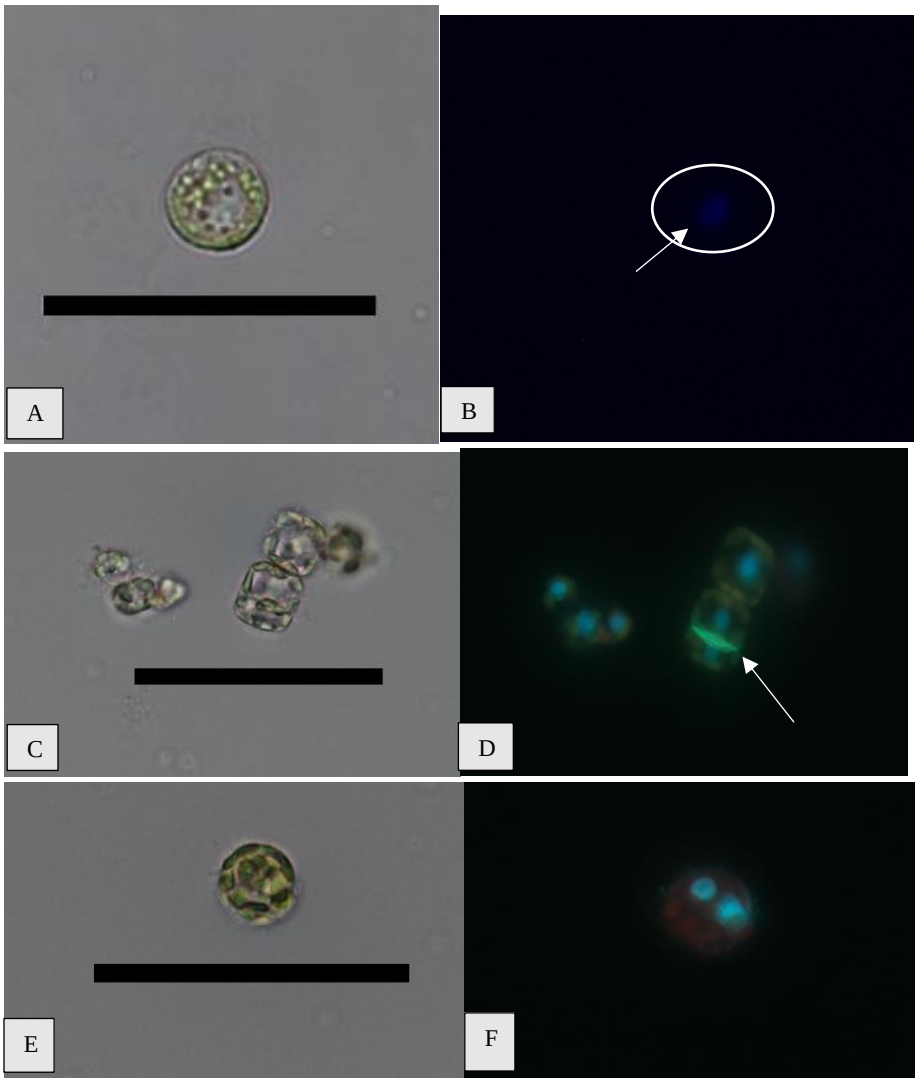

Figure 4. Atypical cells observed in *T. nordenskioeldii* using induction protocols I and II using LM (A, C, E, G) and ELM (B, D, F, H). **A, B** Spherical cell with 1 nucleus (as indicated with arrow and circle). **C, D** A vegetative dividing cell that is producing a new valve whose silica is traced by PDMPO (shown by arrow). **E, F** Cell with 2 nuclei. Scale bare = 50 µm.

Size Classes

There was an observed response in *T. nordenskioeldii* to the induction. The average valve diameter was significantly larger after induction, than before (P=1.32E-13, Table 5). The observed range for cell diameter was wide, ranging from 9.9 µm to 76.6 µm (SE=1.9). Two distinct classes were observed. The typical 'vegetative' cells (small) and the larger 'spherical' cells (Fig. 5). Valve diameter of the induced population was 20.4 µm ± 13.6 S.D., which is larger

than when the batch culture first arrived and measured for species confirmation. However, the larger spherical cells represented very little of the induced population, only about 12.1%.

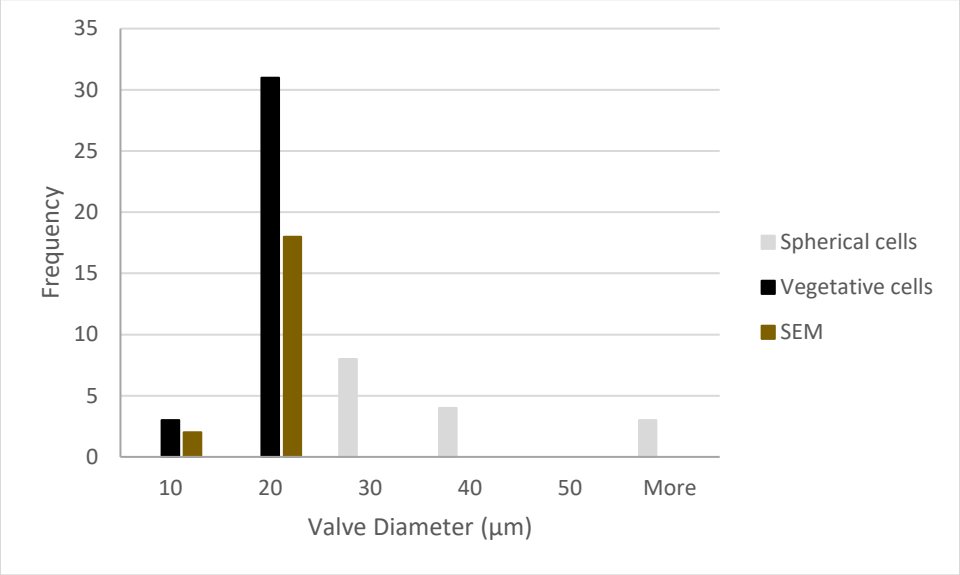

Figure 5. Cell size (µm) of *T. nordenskioeldii* in population upon arrival to the lab from SEM images (SEM) and post-induction using protocol III from LM images. Bin ranges of 10 µm for both vegetative and spherical cells displaying two distinct cell types, small 'vegetative cells' and large 'spherical cells' (N=50).

Structural Elements of Enlarged Cell walls

The large vegetative cells were examined using SEM. These enlarged cells range from 14-23 µm in diameter and correspond to the second "vegetative size class on Fig. 5. They show some of the species-specific characteristics of this species, similar to the smaller vegetative cells examined before induction. They show the fultoportula, girdle band and radial areolation (Fig 6). However, these cells seemed to have been weakly silicified, and collapsed on each other in CPD SEM preparations (Fig 6, A-B).

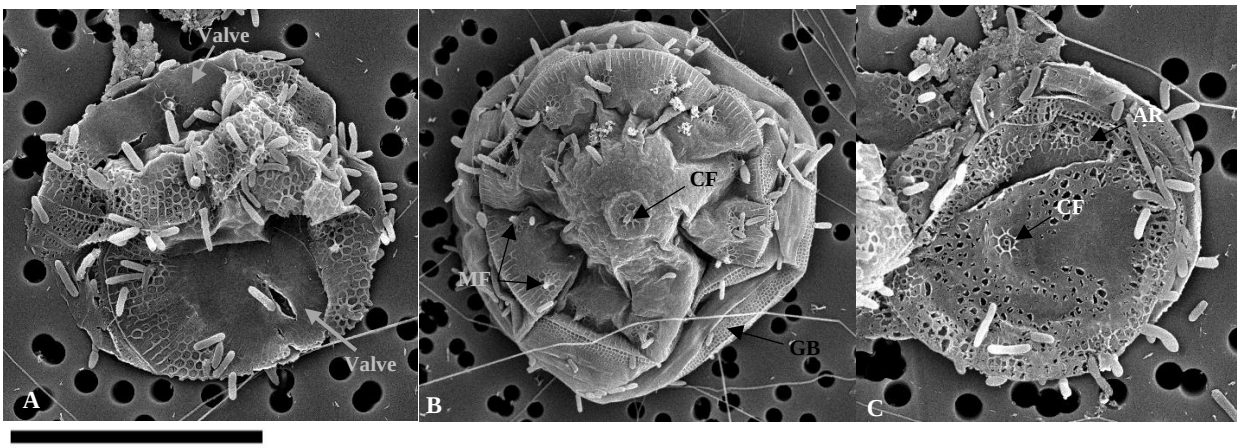

Figure 6. SEM images of *T. nordenskioeldii* valves' of large cells from protocol II (A,B,C). **A**, A frustule lying on the girdle side with valves folded towards each other. **B**, Collapsed large cell with some of the valve morphology characteristic specific to the species. **C**, One valve of a large cell with distinct, near normal valve morphology. MF = Marginal fultoportula, CF = central fultoportula, GB = Girdle band, AR = areolation. Scale bare = 10 µm

4.3 Induction of *T. weissflogii*

Cell Types

Following induction protocols III and IV, a number of atypical cells appeared, although no gametogenesis or mature auxospores were observed. The two types of atypical cells observed post-induction were: spherical (free in the growth medium and attached to a parental frustule) with strongly concentrated plastids and large colorless remainder of the cell (Fig 7, A-B), and cells of various sizes with irregular shapes and great number of dispersed chloroplasts (Fig 7, C-D). One cell that resembles an auxospore (58.6 µm) was observed early on in the experimental trials, however only one cell like this was observed throughout the entire experiment (Fig 7, F).

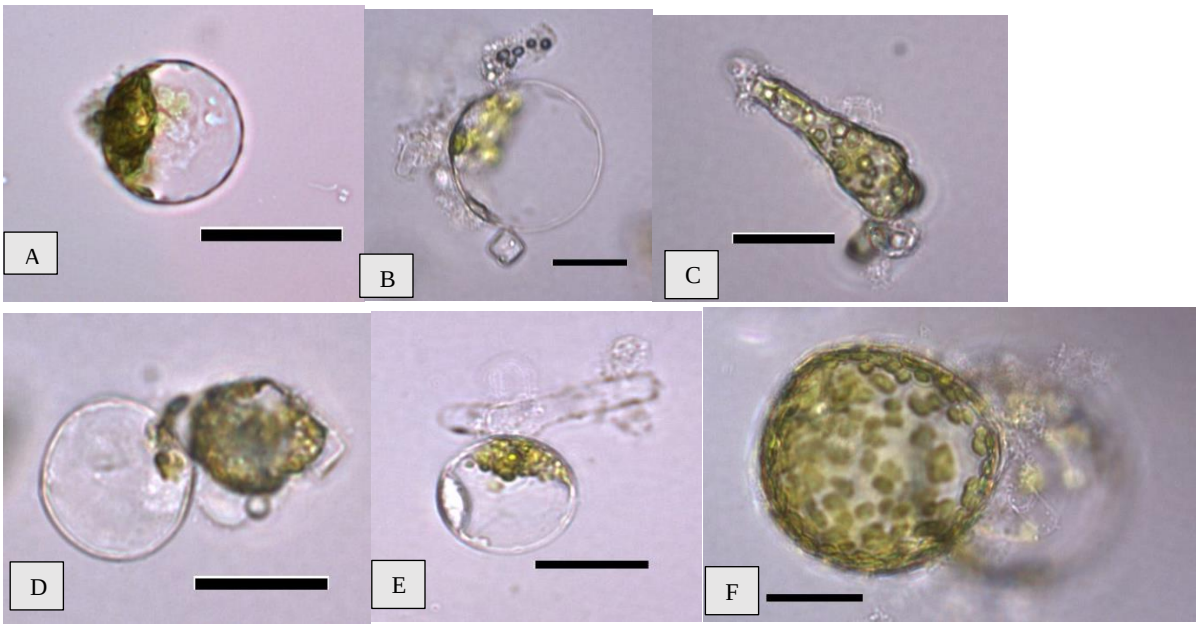

Figure 7. Types of cells found in *T. weissflogii* after induction protocols III and IV. (A and B) Spherical cells with strongly concentrated plastids. (C and D) Irregular cell development with dispersed chloroplasts. (E) Protoplast inflation and cell enlargement. (F) Cell with morphology similar to an auxospore. Scale bar = 25.

Epifluorescence microscopy *T. weissflogii* shown that many of the irregular cells observed were multinucleated, ranging from 2-5 nuclei within a cell (Fig 8). The nucleus in some of the images are difficult to observe due to the lack of contrast in the image and therefore, such images are easier to observe in the dark (Fig 8, J).

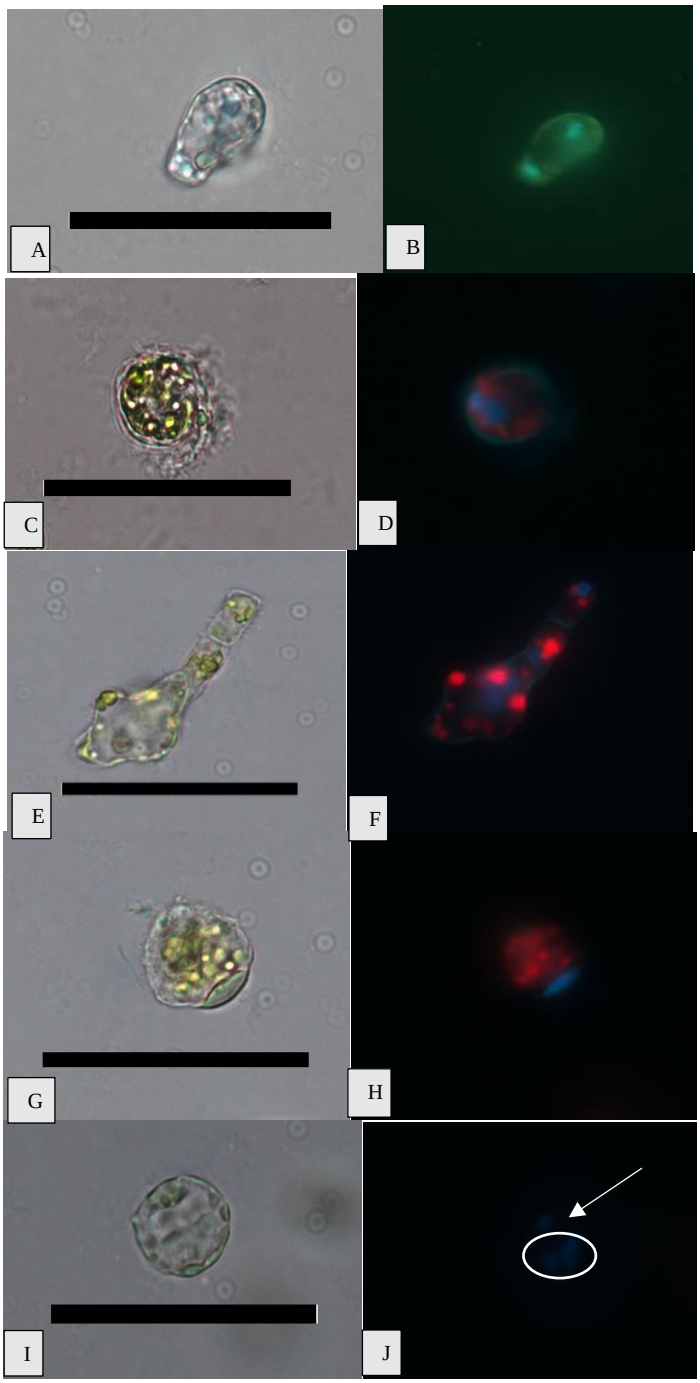

Figure 8. Irregular shaped cells observed in *T. weissflogii* following the induction protocol III, using LM (A, C, E, G, I) and ELM (B, D, F, H, J) of the same cell. **B**, dividing cell 2 nuclei that are separated. **D**, enlarging cell with 2 nuclei and silica wall. **F**, irregular shape cell with 3 nuclei. **H**, enlarging cell with one large nucleus and non-siliceous wall. **J**, large multinucleated cell with at least 5 nuclei, the circle showing a group of about 4 and the arrow showing a singular nucleus. Scale bar = 50 µm.

Cell Size Classes

A wide range of cell sizes was observed in *T. weissflogii*, however, there was no signs of sexualization in the form of oogenesis, spermatogenesis or mature auxospores with initial cells inside. In the modified media, following the Moore et al. (2017) protocol (Protocol III) a wide range of cell sizes for vegetative and spherical cells ranged from 5.2 µm – 69.7 µm (SE=1.94). The average cell diameter was significantly higher (P=6.47E-08) after induction when compared to the average cell size of the batch cultures when they arrived in lab for SEM confirmation, according to a T-test of unequal variances. In the graph below, all three different cell types, vegetative, spherical and irregular cells were organized by cell size and arranged in size classes (Fig. 5). The mean valve diameter was 24.8 µm ± 24.8 S.D. These irregular cells were rare, only occurring in about 17% of the population, however, the spherical cells were rarer, about 10% of the population.

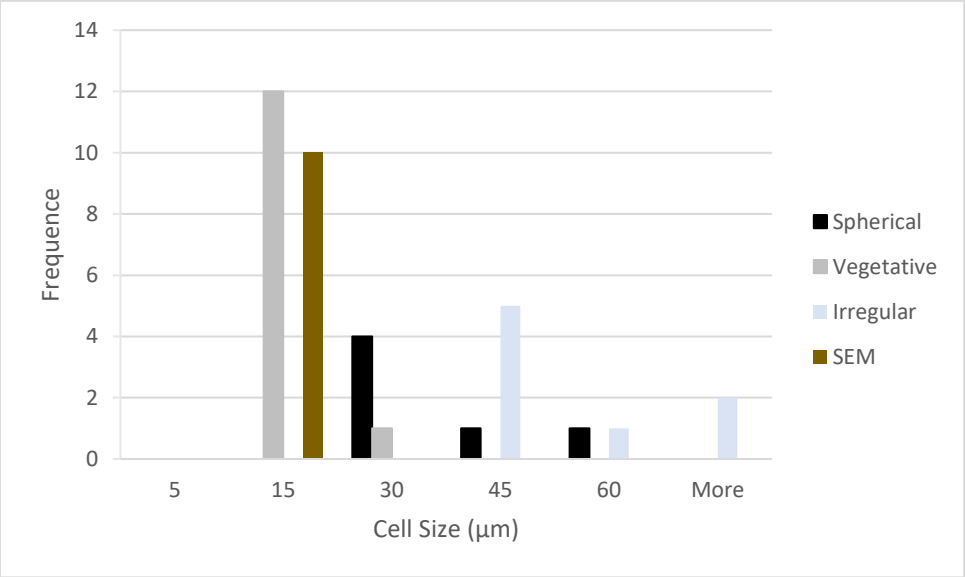

Figure 9. Cell size (µm) of *T. weissflogii* in population upon arrival to the lab from SEM images (SEM) and post-induction using protocol III from LM images. Bin ranges of 15 µm for both vegetative and enlarged cells displaying three distinct cell types, ‘vegetative cells’, ‘spherical cells’, and ‘irregular cells’ (N=75).

Structural Elements of Enlarged Cell walls

Three different types of large vegetative cells were examined using SEM: long, slightly silicified cells (16-35 µm), cells that resemble oogonia (18-24 µm), and bulged, highly silicified

cells (20-40 µm) (Fig 10). The ‘long, lightly silicified’ cells had bands in the long girdle that had valve face characteristics, mainly areolae (Fig 10, A-B). The oogonia shaped cells had a small bulge (Fig 10, C, compare to Fig. 1 b & c)) and according to EDS, it was lightly silicified as the silica peak from the energy peak graph was small (Fig 10, E). The long, bulged cells (Fig 10, D) were highly silicified as shown in the energy peak graph from the EDS (Fig 10, F).

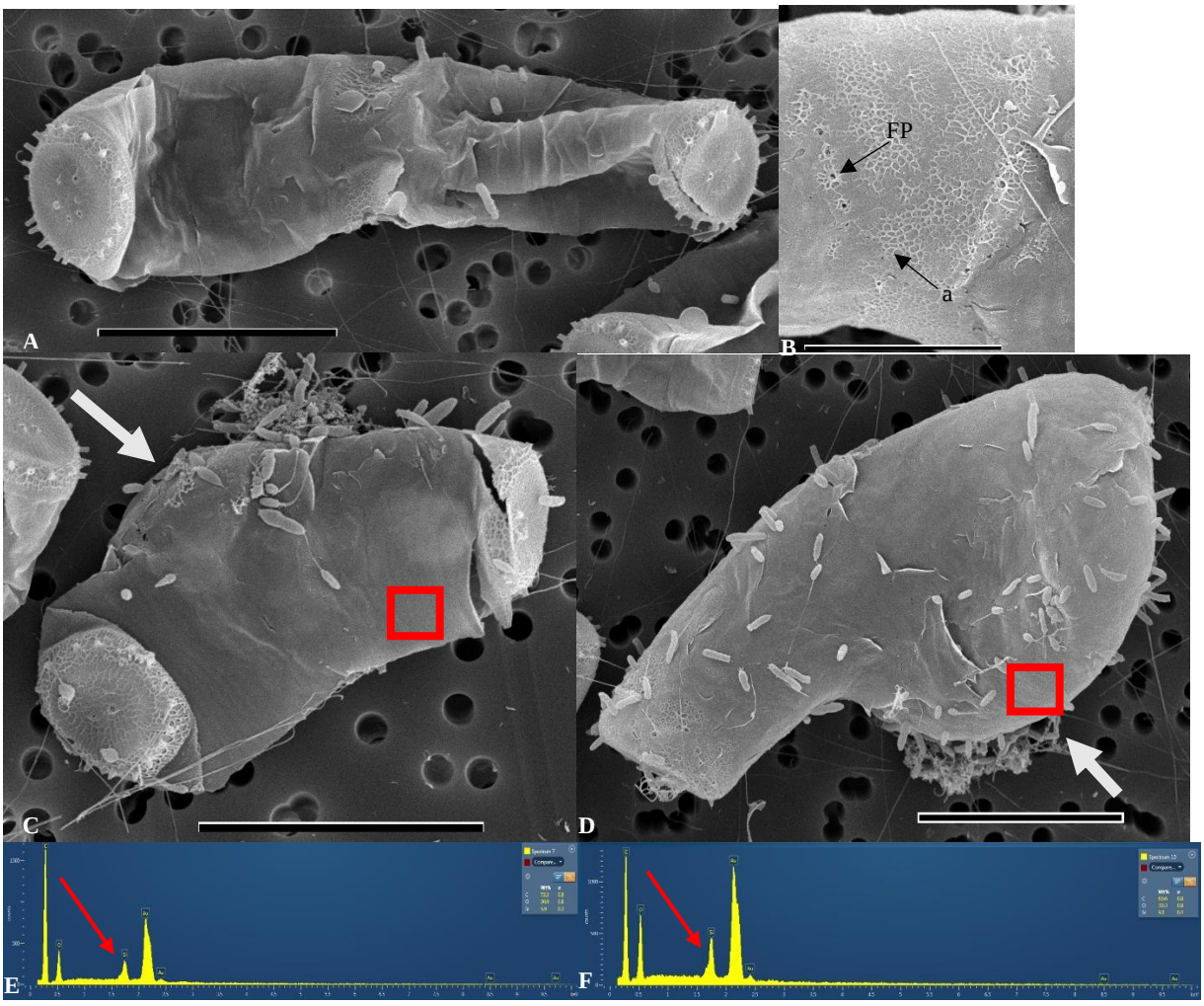

Figure 10. Representative SEM images of types of large vegetative cells observed, with corresponding EDS peak energy graphs, using protocol III. **A**, Long, weakly silicified cell. **B**, Areolae (a) and fultoportula (FA) in arranged in a band on large vegetative cells. **C**, Vegetative cell in the shape of a young oogonia, that is slightly bulged (arrow). D, Large, highly silicified cell that is bulged (arrow), but is not resembling an oogonium. Red squares (C-D) correspond to areas examined in EDS corresponding to the energy peak graph below. **E**, Energy peak graph for oogonia like cell (C). **F**, Energy peak cell for silicified bulged cell. E-F, Red arrow points to silica energy peak. Scale bare = 10 µm.

4.4 Induction of *Thalassiosira* cf. *oceanica*

Cell Types

The induction protocols III and IV of *Thalassiosira* cf. *oceanica* was unsuccessful since no gametogenesis, auxospores, enlargement or irregular cells were not observed, except for one case. In the span of two months and two different sexual induction protocols, only one atypical cell was observed (Fig 10). It was a large (24 µm) free spherical cell with concentrated chloroplast, and therefore accounted for less than 1% of the population.

Figure 11. The only large spherical cell observed in *T.* cf. *oceanica* post-induction. Scale bar=25 µm.

Size Classes

The average cell size within the population after induction was 4.8 µm (SD=0.96, N=43), which was well below the maximum cell size. Furthermore, no distinct class sizes were observed after any of the sexual inductions (Fig 11).

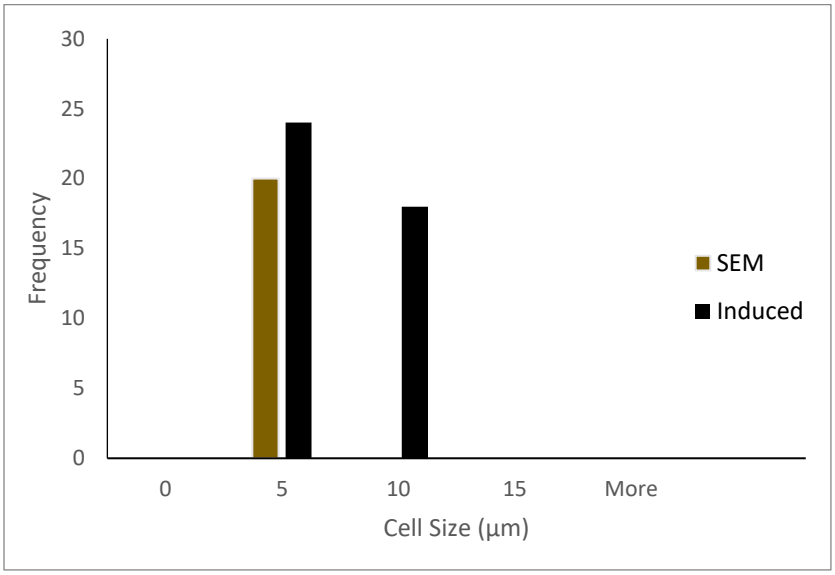

Figure 12. Cell size (µm) of *T.* cf. *oceanica* in population upon arrival to the lab from SEM images (SEM) and post-induction using induction protocol III from LM images (Induced). Bin ranges of 5 µm. Cells ranged in size from 3.3 µm to 8.2 µm (N=63).

5 Discussion

5.1 Spherical Auxospores and Cells

T. nordenskioeldii and *T. weissflogii*

Spherical auxospores are commonly observed in non-polar centric diatoms, e.g. *Actinocyclus* (Idei et al. 2012). These auxospores expand isometrically, hence their spherical shape (Chepernov et al. 2018). During the auxospore expansion, the thecae of the oogonium remains attached to the opposite sides of the auxospores, looking like two caps. Another characteristic that is typically observed in these auxospores are a complete covering of thick siliceous scales which can be observed using SEM (Idei et al. 2012). After expansion, the auxospore has formed an initial cell, however, the initial cell is still enclosed in the auxospore membrane (Chepernov et al. 2018; Chepernov et al. 2012). Therefore, spherical auxospores and their resulting initial cells have a distinct morphology.

The spherical cells observed in both *T. nordenskioeldii* and *T. weissflogii*, however, did not have typical auxospore morphology. The attached thecae were absent near the spherical cells, and in *T. nordenskioeldii* the cell walls had little silica deposition with no scales. In *T.*

weissflogii, some of the larger cells were heavily silicified but were not spherical. Furthermore, cells that resembled oogonia were observed in SEM and the presence of multinucleated cells which suggests that some form of gametogenesis occurred. Despite this, initial cells were produced suggesting that sexualization was not completed. The frequency of binucleated cells (putative primary oocytes) observed suggests either Type 1 or 2 oogenesis might be present, however, since spermatogenesis was absent it is most likely that the eggs remained unfertilized and eventually aborted. This was similar to what was observed in *T. nordenskioeldii,* however, binucleated cells were rarely observed in this clone. Nonetheless, cells that resembled disintegrating oocyte or egg cells were observed. Since spermatogenesis was not observed it is likely, as seen in *T. weissflogii*, that full sexual process did not take place, and the putative oocytes aborted.

In many centric non-polar diatoms, the spherical auxospores develop from the fertilized egg as a result of oogamous reproduction. However, due to the lack of spermatogenesis and the obvious presence of oogonia, the spherical cells observed here may not be products of oogamy, nor true auxospore cells. However, in *T. weissflogii*, a cell that resembled an auxospore was observed. The presence of possible auxospores without any signs of spermatogenesis suggest that autogamy may also be possible. The multinucleated cells observed in *T. weissflogii* were similar to those observed by Mills and Kaczmarska (2006) in *Thalassiosira angulate*, which reproduces via autogamy. Such cells include a possible tri-nucleated auxospore mother cell and a binucleated auxospore, in the early stage before mitotic division, and both tri-nucleated and bi-nucleated cells were observed in *T. weissflogii*. However, no auxospores with initial cells were observed, which suggests that auxosporulation was not completed. Since no mature auxospores or initial cells were documented in the cultures of *T. weissflogii* by other researchers (Moore et al. 2017), I suggest that auxsoporulation might have not occurred neither in my nor their clones.

There are a few reasons why the induction may not be successful. One of which could be due to fact that the clone cells lost its capacity to sexualize. This has been observed in some clonal cultures harboring exceptionally small cells, near or below the cl size ranges known from natural populations. This certainly may apply to all the clones used in this study. It is equally likely may also be that Moore et al. (2017) misinterpreted their “auxospore” cells. In Moore et al. (2017) no representative cells of mature auxospores in *T. weissflogii* were documented (as is the

case in my results). Only one image was shown to represent an auxospore by Moore et al. (2017), and it is quite different from typical immature auxospores shown by Chepurnov et al. 2018 documenting entire sexual cycle in *T. weissflogii*. Moore et al (2017) "auxospore" images are very similar to cells I observed, and these had not been observed to culminate their development in initial cell. Finally, Moore et al. (2017) protocol for *T. weissflogii* sexualization was lacking clarity and so it is possible that I could not replicate it because some critical factors was misinterpreted.

Reproduction and cell enlargement in *T. nordenskioeldii* suggest that sexual reproduction did not occur in the conditions that were tested, which were periods of high light to no light with warmer and colder temperatures. Perhaps a different light and dark cycle was needed since this species prefers the colder waters near the arctic, which has greater variations in daylight exposure due to the seasonality (i.e. more daylight in the summer versus the winter). However, while no sexual reproduction was observed, a large range of size classes were observed with a larger cell size post-induction, therefore suggesting that some form of enlargement occurred. Though while some size classes observed were larger post-induction, there was a size class that was like the cell size before induction for both in *T. nordenskioeldii* and *T. weissflogii*. This smaller size class is most likely the critical size threshold, which is the size in which the sexual cycle can be induced. Sizes above this threshold cannot be induced to undergo sexual reproduction, whereas cells below are able to (Von Dassow et al. 2006). For example, the smallest size class observed for *T. weissflogii* was 5-9 µm, which is below the calculated threshold of 9.9 µm from a recent study on the sexual life cycle of this clone (Von Dassow et al. 2006). Therefore, sexualization could have occurred during the induction. A similar trend was observed in *T. nordenskioeldii,* however the sexual cycle of this clone has yet to be described in the literature, so it is difficult to suggest that sexualization may have occurred. However, since these inflated cells had no attached frustules, it is highly likely that these cells were viable. Often under the light microcopy, these cells were often observed degenerated or deformed. Perhaps, the lack of frustule and the consequent lack of silica is the cause for the lack of viability of the cell. In fact, some studies have shown that these frustules can protect the DNA of the cell, as the silica in these frustules can reflect UV light (Aguirre et al. 2018). The auxosporulation of *T.*

nordenskioeldii has yet to be described, however, it is likely to be oogamous due to a presence of aborted oocytes.

T. cf. oceanica (PicoThala)

No sexualization, auxosporulation or irregular cells were observed in the experimental flasks. There are many different reasons as to why *T.* cf. *oceanica* was not able to sexualize, perhaps there was a cue missing in my induction. *T. oceanica* is an oceanic diatom and has a different photoadaptation than other diatoms, such as T. *nordenskioeldii,* that live in neritic habits (Hasle 1983). Therefore, this clone is well adapted to lower light intensities and it is well adapted to low nutrients, as it is an open ocean diatom, which is perhaps why attempting to induce with a nutrient limitation did not work. Another possible reason as to why this clone did not reproduce sexually, or enlarge, is that this clone lost its sexuality. Loss of sexuality in clonal flowering plants is commonly observed, and soon populations can become obligate asexuals (Barrett 2015). While common in terrestrial plants, it has only been observed in a handful of diatom species, *T. pseudonana* being best known example. However, the limited number of examples showing this loss of sexuality in diatom species could be due to lack of research in this field of study (Koester et al. 2018). The loss of sexuality most likely occurs due to a gene loss and lack of genetic diversity caused by frequent asexual reproduction and is common in clonal cultures (Koester et al. 2018). Therefore, it is possible that this may some of the clonal cultures in the lab may have lost their sexuality.

5.2 Size Classes and Vegetative Cell Enlargement

T. cf. oceanica (PicoThala)

When the clones were measured upon arrival to the lab, prior to induction, only one size class was observed for each clone. After induction, however, more than one size class was observed in all clones. *T.* cf. *oceanica* only had two vegetative cell size classes observed post-induction. There was little change in cell size observed in *T.* cf. *oceanica* as cell sizes above 8 µm were never observed post-induction. However, it is still considered an increase in size from what was observed in SEM which was approximately 4 µm. This increase in cell size could be a result of vegetative cell enlargement, however, irregular cells like those observed in the other two clones were rarely observed. Therefore, suggesting that vegetative enlargement did not commonly occur

during or after induction. This size increase is most likely due to other factors, such as a larger sample size as well as the difference in measurement methodology, as the cell size is measured post-induction by using LM which is less accurate than SEM, which was used to measure prior to induction. Due to a lack of irregular cells observed during induction (with only one spherical cell observed), there is little evidence to suggest that vegetative enlargement occurred post-induction.

T. nordenskioeldii

Thalassiosira nordenskioeldii, in contrast to *T.* cf. *oceanica*, has a range of size classes observed post-induction. Two size classes for vegetative cells, the second (larger) class had a cell size more than 20 µm, which is nearly double of what was observed pre-induction. There were at least two size classes for enlarged cells observed post-induction. One of which was 50 µm or more, which were rather rare, while the most common size class for enlarged cells (smaller) was between 30-49 µm. Both size classes included large spherical cells, which accounted for the observed cell size increase post-induction even though these cells were not common, representing only about 12% of the population. However, these spherical cells may not be viable due to the lack of silica in the cell walls. This could explain why these cells were rarely observed above a specific cell size (approximately 60 µm), as observations under LM suggest the spherical cells inflated until they became unviable and burst. In conclusion, the cell size increase observed post-induction is most likely a form of unsuccessful vegetative cell enlargement, perhaps species-specific enlargement, providing only a temporary increase in cell size.

T. weissflogii

Thalassiosira weissflogii had a similar response to *T. nordenskioeldii*, in which there was three or more size classes observed, including the spherical cells with two size classes. However, an additional cell type, the irregular cells, that were observed in *T. weissflogii* but not *T. nordenskioeldii.* These irregular cells accounted for the largest size class (59 µm or more). However, the two vegetative size classes (small and large) and two enlarged size classes (small and large) were very similar to *T. nordenskioeldii.* Since it is unlikely that the spherical cells were viable, or at the least had a low survival rate, as those observed in *T. nordenskioeldii*, the irregular cells most like the sources of the larger cells in the population. However, despite this, the spherical cells were represented in the populations by 10% and therefore, accounted for the

increase in the cell size post-induction. The spherical cells observed in *T. weissflogii* are similar those observed in *T. nordenskioeldii* as temporary increase in cell size post-induction. However, the irregular cells contributed to a more stabilized increase in cell size. These irregular cells were highly silicified and bulged, and most likely a form of vegetative cell enlargement in *T. weissflogii.* The spherical cells that are observed in both *T. nordenskioeldii* and *T. weissflogii* were some form of vegetative enlargement, perhaps species-specific since these types of cells were not well-recorded in literature. Therefore, due to lack of typical auxospores and no observed spermatogenesis suggests that *T. weissflogii* used alternative means to reintroduce cell size to the population instead of auxosporulation.

6 References

Aguirre LE, Ouyang L, Elfwing A, Hedblom M, Wulff A, Inganäs O (2018) Diatom frustules protect DNA from ultraviolet light. Sci Rep 8:1-6

Barrett SC (2015) Influences of clonality on plant sexual reproduction. PNAS 112:8859-8866

Chepurnov VA, Mann DG, Sabbe K, Vyverman W (2004) Experimental studies on sexual reproduction in diatoms. Int Rev Cytol Supl 237:91-154

Chepurnov VA, Mann DG, Von Dassow P, Armbrust EV, Sabbe K, Dasseville R, Vyverman W (2006) Oogamous Reproduction, with two-step Auxosporulation in the centric diatom Thalassiosira punctigera (Bacillariophyta) J Phycol 42:845-858

Chepurnov VA, Chaerle P, Vanhoutte K, Mann DG (2012) How to breed diatoms: Examination of two species with contrasting reproductive biology. In Algal Res, 323-340, Springer, Dordrecht

Chepurnov VA, Steigüber C, Siegel P (2018) Diatoms as hatchery feed: on-site cultivation and alternatives. Hatcheryfeed 6:23-27

Davidovich NA, Davidovich OI, Podunay YA, Gastineau R, Kaczmarska I, Poulíčková A, Witkowski A (2017) Ardissonea crystallina has a type of sexual reproduction that is unusual for centric diatoms. Sci Rep 7:14670.

Godhe A, Kremp A, Montresor M (2014) Genetic and microscopic evidence for sexual reproduction in the centric diatom Skeletonema marinoi. Protist 165:401-416

Guillard RRL (1975) Culture of phytoplankton for feeding marine invertebrates. In: (W.L. Smith and M.H. Chanley, eds.) Culture of marine invertebrate animals. Plenum Press, New York. pp. 26–60.

Hasle GR (1983) The Marine, Planktonic Diatoms Thalassiosira Oceanica sp. nov. and T. Partheneia. J Phycol 19:220-229

Idei M, Osada K, Sato S, Toyoda K, Nagumo T, Mann DG (2012) Gametogenesis and auxospore development in Actinocyclus (Bacillariophyta). PLoS One 7(8)

Kaczmarska I, Ehrman JM, Bates SS (2001) A review of auxospore structure, ontogeny and diatom phylogeny. In Proceedings of the 16th international diatom symposium pp 153-168

Kaczmarska I, Medlin LK (2004) Evolution of the diatoms: V. Morphological and cytological support for the major clades and a taxonomic revision. Phycologia 43:245-270

Kaczmarska I, Poulíčková A, Sato S, Edlund MB, Idei M, Watanabe T, Mann DG (2013) Proposals for a terminology for diatom sexual reproduction, auxospores and resting stages. Diatom Res 28:263-294

Koester JA, Berthiaume CT, Hiranuma N, Parker MS, Iverson V, Morales R, ... & Armbrust EV (2018) Sexual ancestors generated an obligate asexual and globally dispersed clone within the model diatom species Thalassiosira pseudonana. Sci Rep 8:1-9

Manton I (1966) Observations on the fine structure of the male gamete of the marine centric diatom Lithodesmium undulatum. J R Microsc Soc 85:119-134.

Medlin LK (2016) Evolution of the diatoms: major steps in their evolution and a review of the supporting molecular and morphological evidence. Phycologia 55:79-103

Mills KE, Kaczmarska I (2006) Autogamic reproductive behavior and sex cell structure in Thalassiosira angulata (Bacillariophyta). Bot Mar 49:417-430

Mizuno M (2006) Evolution of meiotic patterns of oogenesis and spermatogenesis in centric diatoms. Phycol Res 54:57-64

Mizuno M (2008) Evolution of centric diatoms inferred from patterns of oogenesis and spermatogenesis. Phycol Res 56:156-165

Moore ER, Bullington BS, Weisberg AJ, Jiang Y, Chang J, Halsey KH (2017). Morphological and transcriptomic evidence for ammonium induction of sexual reproduction in Thalassiosira pseudonana and other centric diatoms. PloS one, 12(7)

Round FE, Crawford RM, Mann DG (1990). The Diatoms. Cambridge University Press, Cambridge, 741 p

Samanta B, Kinney ME, Heffell Q, Ehrman JM, Kaczmarska I (2018) Gametogenesis and auxospore development in the bipolar centric diatom Brockmanniella brockmannii (family Cymatosiraceae). Protist 168:527-545

Schultz ME, Trainor FR (1970) Production of male gametes and auxospores in a polymorphic clone of the centric diatom Cyclotella. Can J Bot 48:947-951

Stachura-Suchoples K, Williams DM (2009). Description of *Conticribra tricircularis*, a new genus and species of Thalassiosirales, with a discussion on its relationship to other continuous cribra species of *Thalassiosira* Cleve (Bacillariophyta) and its freshwater origin. J of Phycol 44: 477-486

Tomas CR, eds (1997) Identifying marine phytoplankton. Academic Press, 858 p

von Stosch HA (1982) On auxospore envelopes in diatoms. Bacillaria 5:127–156

Von Dassow P, Chepurnov VA, Armbrust EV (2006) Relationships Between Growth Rate, Cell Size, and Induction of Spermatogenesis in the Centric Diatom Thalassiosira weissflogii (Bacillariophyta) 1. J of Phycol 42:887-899

Znachor P, Nedoma J (2008) Application of the PDMPO technique in staining silica deposition in natural populations of Fragilaria corotenisis (Bacillariophyceae) at different depths in eutrophic reservoir. J of Phycol 44:518-525